



Original Article

Diagnostic Performance of Magnetic Resonance Imaging for Vertebral Metastases in Routine Clinical Practice

Laila Khan¹, Zubair Janan Orakzai^{1*}, Tabassum Begum¹, Hina Baig¹, Sumaira Nooreen¹ and Muhammad Sadiq¹

¹Department of Radiology, Bacha Khan Medical College, Medical Teaching Institute, Mardan Medical Complex, Mardan, Pakistan

ARTICLE INFO

Keywords:

Spine MRI, Vertebral Metastasis, Diagnostic Accuracy, Histopathology, Tumor Board Consensus, ROC Curve

How to Cite:

Khan, L., Orakzai, Z. J., Begum, T., Baig, H., Nooreen, S., & Sadiq, M. (2026). Diagnostic Performance of Magnetic Resonance Imaging for Vertebral Metastases in Routine Clinical Practice: MRI Diagnostic Performance for Vertebral Metastases in Routine Practice. *Pakistan Journal of Health Sciences*, 7(4), 111-118. <https://doi.org/10.54393/pjhs.v7i4.3830>

***Corresponding Author:**

Zubair Janan Orakzai
Department of Radiology, Bacha Khan Medical College, Medical Teaching Institute, Mardan Medical Complex, Mardan, Pakistan
zjaurakzai@hotmail.com

Received Date: 15th January, 2026

Revised Date: 14th February, 2026

Acceptance Date: 3rd March, 2026

Published Date: 30th April, 2026

ABSTRACT

Vertebral metastasis is a frequent complication of systemic malignancies and may cause pain, pathological fractures, and neurological compromise. MRI is commonly used for suspected spinal metastases; however, the diagnostic performance of routine 1.5-Tesla MRI interpreted using visual criteria in everyday practice remains unclear. **Objectives:** To determine the diagnostic accuracy of conventional MRI for the detection of vertebral metastases using histopathology and/or multidisciplinary clinic radiologic consensus as reference standards. **Methods:** This prospective cross-sectional study at MTI Bacha Khan Medical College and Mardan Medical Complex, Pakistan (15 Sept–15 Dec 2025), included 106 adults with suspected vertebral neoplastic lesions who underwent 1.5-Tesla MRI. Two blinded radiologists independently interpreted scans, resolving discrepancies by consensus. Histopathology and/or tumor board consensus served as the reference standard. Sensitivity, specificity, predictive values, accuracy, and ROC-AUC were calculated. **Results:** Of 106 patients, 64 (60.4%) had vertebral metastases by the reference standard. MRI sensitivity was 42.2% (95% CI: 30.1–54.3), specificity 54.8% (95% CI: 39.7–69.9), PPV 58.7% (95% CI: 44.5–72.9), NPV 38.3% (95% CI: 26.1–50.5), and overall accuracy 47.2% (95% CI: 37.7–56.7). The AUC was 0.515 (95% CI: 0.40–0.63). False positives were commonly due to hemangioma and infection, whereas false negatives were mainly related to poor image quality, small/early lesions, and reader variability. **Conclusions:** Conventional 1.5-Tesla MRI using routine visual criteria showed low sensitivity, modest specificity, and limited accuracy for vertebral metastases. Clinical correlation and reference-standard confirmation remain essential for equivocal cases.

INTRODUCTION

Vertebral metastasis represents the most common form of malignant involvement of the skeletal system and constitutes a major cause of morbidity, chronic pain, neurological compromise, and reduced quality of life in patients with systemic malignancies [1]. The spine is particularly vulnerable to metastatic spread because of its rich vascular supply and high content of red marrow, making it a frequent site of secondary tumor deposits. Early and accurate detection of vertebral metastases is therefore critical, as delayed diagnosis may result in irreversible spinal cord compression, pathological fractures, and permanent neurological deficits. Timely

identification plays a central role in guiding therapeutic decisions, including surgery, radiotherapy, and systemic treatment, and directly influences patient outcomes [2]. Magnetic resonance imaging (MRI) is widely regarded as the imaging modality of choice for the evaluation of suspected vertebral metastases, owing to its superior soft-tissue contrast, multiplanar capability, and high sensitivity for detecting early bone marrow infiltration before cortical destruction becomes apparent on conventional radiography or computed tomography [3]. Typical MRI features of vertebral metastases include T1 hypointensity, T2/STIR hyperintensity, diffusion restriction, contrast



enhancement, and involvement of the pedicles or posterior elements. However, despite these established imaging criteria, considerable overlap exists between metastatic lesions and a range of benign conditions, including vertebral hemangiomas, infectious spondylitis, osteoporotic compression fractures, and degenerative Modic changes. This overlap often leads to diagnostic uncertainty and may result in inappropriate management if imaging findings are misinterpreted [4, 5]. In recent years, advanced techniques such as quantitative diffusion-weighted imaging, radiomics, and artificial intelligence-assisted image interpretation have shown promising improvements in the diagnostic performance of MRI [6, 7]. Nevertheless, in most low- and middle-income settings, including Pakistan, routine clinical practice continues to rely predominantly on conventional visual interpretation of standard MRI sequences. There is limited real-world evidence regarding the diagnostic accuracy of such routine MRI protocols in differentiating metastatic from non-metastatic vertebral lesions, particularly in South Asian populations, where patterns of primary malignancies and access to advanced imaging tools may differ from those reported in high-income countries [8]. This evidence gap is directly relevant to the scope of radiology-focused journals, which emphasize evaluating imaging performance in routine clinical practice. The study hypothesized that conventional MRI, when interpreted using standard visual criteria alone, has limited diagnostic accuracy for differentiating metastatic from non-metastatic vertebral lesions in routine clinical practice. Therefore, the present study was designed to evaluate the diagnostic accuracy of conventional 1.5-Tesla MRI for the detection of vertebral metastases using histopathology and multidisciplinary clinic radiologic consensus as reference standards, and to analyze the causes of diagnostic discordance in routine reporting. The study aimed to provide clinically relevant evidence aligned with the journal's focus on diagnostic imaging performance and quality of radiologic interpretation.

METHODS

The study was a prospective cross-sectional diagnostic accuracy study (diagnostic test evaluation) conducted at the Department of Radiology, MTI Bacha Khan Medical College and Mardan Medical Complex, Mardan, Pakistan, over three months (15 September 2025 to 15 December 2025) after ethical approval by the Ethical Review Board of Bacha Khan Medical College, Mardan (Approval No. 929/BKMC). Ethical clearance was granted for the research project entitled "Diagnostic Accuracy of Magnetic Resonance Imaging for Vertebral Metastases." Written informed consent was obtained from all participants before enrollment, and the study was carried out in

compliance with the Declaration of Helsinki. The study was conducted and reported in accordance with the Standards for Reporting Diagnostic Accuracy Studies (STARD 2015) guidelines. All clinical and imaging data were anonymized and coded to ensure patient confidentiality. The eligible patients presenting during the study period were enrolled consecutively and underwent MRI followed by reference standard confirmation. Non-probability consecutive sampling was used to enroll one hundred and six (106) adult patients with suspected vertebral lesions on clinical or radiologic grounds between 15 September 2025 and 15 December 2025. Patients aged 18 years and older who presented with vertebral lesions suspicious for neoplastic pathology on initial imaging and proceeded to undergo MRI followed by confirmatory diagnostic reference investigations were eligible. Patients were excluded in case of recent vertebral trauma, a known history of primary spinal infection, poor-quality MRI scans that were non-diagnostic, or incomplete clinical or histopathological data. The sample size was calculated for estimation of MRI sensitivity using the standard single-proportion formula. The sample size was calculated for estimation of MRI sensitivity using the standard single-proportion formula: $n = Z^2 \times S(1 - S) / d^2$, where $Z = 1.96$ for a 95% confidence interval, S was the anticipated sensitivity (70%) based on previously published meta-analytic data on skeletal metastases detection and d was the allowable margin of error (9%) [9]. Every patient underwent MRI examination on a 1.5-Tesla scanner using a standardized spine imaging protocol that comprised sagittal T1-weighted sequences, axial T1-weighted sequences, sagittal T2-weighted sequences, STIR sequences, diffusion-weighted imaging (DWI), and post-contrast fat-suppressed T1-weighted sequences. Two consultant radiologists (each with ≥ 5 years post-fellowship experience) independently interpreted all MRI examinations while blinded to the reference standard outcome. Disagreements were resolved in a joint consensus session to generate the final MRI classification used for analysis. Formal interobserver agreement statistics (e.g., Cohen's kappa) were not calculated, as the final diagnostic classification was based on consensus interpretation; therefore, quantitative assessment of interobserver reproducibility was not performed. MRI was classified as positive for vertebral metastasis when one or more predetermined imaging characteristics were detected, including T1 hypointensity, T2/STIR hyperintensity, diffusion restriction, contrast enhancement, heterogeneous enhancement, pedicle involvement, skip lesions, multiple non-contiguous vertebral involvement, marrow replacement patterns, or adjacent disc sparing. MRI positivity was intentionally defined as a composite visual criterion to mirror routine

reporting practice, where radiologists integrate multiple features into an overall impression. Consequently, the study did not perform feature-level diagnostic modeling or assess the independent predictive performance of individual MRI signs. The reference standard was defined as histopathology from vertebral biopsy whenever biopsy was clinically indicated and technically feasible. For patients without histopathology, final classification was determined by a multidisciplinary tumor board (radiology, oncology, spine surgery, and pathology) using a predefined consensus process incorporating imaging findings, clinical course, laboratory results, and follow-up information. This composite reference standard was selected to reflect routine clinical practice; however, it may introduce classification heterogeneity and potential verification bias in cases without tissue confirmation. A structured proforma was used to record demographic characteristics, clinical parameters, imaging features, and final reference standard outcome. Selection bias was minimized through consecutive patient recruitment. Observer bias was controlled by blinded dual-reader interpretation with consensus resolution. Verification bias was minimized by ensuring that all enrolled patients underwent reference standard assessment. However, because histopathology was not available for all participants, partial verification bias and classification heterogeneity cannot be completely excluded. An audit of discordant MRI examinations was performed to identify technical and interpretative factors contributing to false-positive and false-negative results. Statistical analysis was performed using IBM SPSS Statistics version 26.0. Normality of continuous variables was assessed using the Shapiro-Wilk test. Continuous variables were summarized as median and interquartile range, and categorical variables were expressed as frequencies and percentages. Pearson chi-square or Fisher's exact test and the Mann-Whitney U test were used to compare categorical and continuous variables, respectively. Diagnostic performance indices, including sensitivity, specificity, positive predictive value, negative predictive value, overall accuracy, and 95% confidence intervals, were calculated. Receiver operating characteristic (ROC) curve analysis was performed to estimate the area under the curve (AUC), and effect sizes were reported using Cramer's V. A p-value < 0.05 was considered statistically significant.

RESULTS

The two groups were comparable with respect to age and duration of symptoms, with no statistically significant differences observed. The female gender was significantly more frequent in the metastatic group, indicating a possible gender-related difference in disease distribution. No significant associations were identified for age group,

smoking status, presence of back pain, or neurological deficit between the two groups. The baseline demographic and clinical characteristics of patients with and without vertebral metastasis. Additionally, the overall pattern of primary tumors was similar in both metastatic and non-metastatic groups. No statistically significant difference was observed in the distribution of primary tumor types, suggesting that the underlying primary malignancy profile did not differ meaningfully between the two groups. The distribution of primary malignancy types stratified by gold-standard diagnosis. Further, there were no significant differences in vertebral region, number of vertebrae involved, posterior element involvement, paraspinal mass, or epidural extension. Pathological vertebral collapse demonstrated a borderline association with metastatic disease, suggesting a possible trend toward higher fracture risk in metastatic lesions, although this did not reach statistical significance. The comparison of vertebral level involvement and disease extent between the two groups (Table 1).

Table 1: Baseline Demographic and Clinical Characteristics of Patients with and Without Vertebral Metastasis, Distribution of Primary Malignancy Types Stratified and Vertebral Level Involvement and Disease Extent According to Gold-Standard Diagnosis (n=106)

Variables	Metastasis (n=64)	Non-metastasis (n=42)	p-value
Baseline Demographic and Clinical Characteristics			
Age (Years), Median (IQR)	52 (35-68)	53 (36-69)	0.436‡
Duration of Symptoms (Weeks), Median (IQR)	10 (=5-15)	10 (=5-15)	0.933‡
Gender			
Female	37 (57.8%)	16 (38.1%)	0.047*
Male	27 (42.2%)	26 (61.9%)	
Age group			
≤40	11 (17.2%)	12 (28.6%)	0.150
41-60	26 (40.6%)	10 (23.8%)	
>60	27 (42.2%)	20 (47.6%)	
Smoking status			
Smoker	38 (59.4%)	20 (47.6%)	0.234
Non-smoker	26 (40.6%)	22 (52.4%)	
Back pain present	38 (59.4%)	25 (59.5%)	0.988
Neurological deficit	32 (50.0%)	22 (52.4%)	0.810
Primary Tumor Type			
Breast	3 (4.7%)	7 (16.7%)	0.473
Gastrointestinal	8 (12.5%)	7 (16.7%)	
Hematological	10 (15.6%)	5 (11.9%)	
Kidney	7 (10.9%)	5 (11.9%)	
Liver	7 (10.9%)	4 (9.5%)	
Lung	8 (12.5%)	6 (14.3%)	
Prostate	8 (12.5%)	4 (9.5%)	
Unknown / Not detected	13 (20.3%)	4 (9.5%)	

Vertebral Region			
Cervical	11 (17.2%)	12 (28.6%)	0.451
Thoracic	20 (31.3%)	10 (23.8%)	
Lumbar	15 (23.4%)	7 (16.7%)	
Sacral	18 (28.1%)	13 (31.0%)	
Number of Vertebrae Involved			
Single	35 (54.7%)	24 (57.1%)	0.803
Multiple	29 (45.3%)	18 (42.9%)	
Posterior Element Involvement	34 (53.1%)	21 (50.0%)	0.753
Paraspinal Soft-Tissue Mass	33 (51.6%)	22 (52.4%)	0.934
Epidural Extension	36 (56.3%)	20 (47.6%)	0.384
Pathological Collapse/Fracture	26 (40.6%)	25 (59.5%)	0.057

*Chi-square test ‡Mann-Whitney U test

None of the individual MRI features showed a statistically significant difference between the two groups, indicating substantial overlap in imaging appearances. A non-significant tendency toward higher prevalence of adjacent disc sparing was observed in non-metastatic lesions, but this finding did not reach statistical significance. The comparison of MRI signal and enhancement characteristics between metastatic and non-metastatic vertebral lesions, table 2.

ability, as reflected by an area under the curve close to 0.5, indicating that MRI performed only slightly better than chance in distinguishing metastatic from non-metastatic lesions (Table 3).

Table 3: Diagnostic Accuracy of MRI for Detection of Vertebral Metastases Using the Gold-Standard Reference (n=106)

Variables	Gold-standard Metastasis +	Gold-standard Metastasis -	Total	Estimate % (95% CI)
MRI Positive	27 (True Positive)	19 (False Positive)	46	–
MRI Negative	37 (False Negative)	23 (True Negative)	60	–
Total	64	42	106	–
Sensitivity	–	–	–	42.2 (30.1-54.3)
Specificity	–	–	–	54.8 (39.7-69.9)
Positive Predictive Value (PPV)	–	–	–	58.7 (44.5-72.9)
Negative Predictive Value (NPV)	–	–	–	38.3 (26.1-50.5)
Overall Accuracy	–	–	–	47.2 (37.7-56.7)
Area Under the Curve (AUC)	–	–	–	0.515 (0.40-0.63)

Values are presented as percentages with 95% confidence intervals in parentheses

The area under the curve indicates poor discriminative performance, confirming the limited diagnostic utility of MRI when compared with the gold-standard reference. The receiver operating characteristic curve for MRI in the detection of vertebral metastases (Figure 1).

Table 2: Comparison of MRI Signal and Enhancement Characteristics between Metastatic and Non-Metastatic Vertebral Lesions (n=106)

MRI feature	Metastasis n (%)	Non-metastasis n (%)	χ^2 value	p-value
T1 hypointensity	30 (46.9%)	16 (38.1%)	0.80	0.372
T2/STIR hyperintensity	34 (53.1%)	23 (54.8%)	0.03	0.869
Diffusion restriction (DWI)	34 (53.1%)	21 (50.0%)	0.10	0.753
Contrast enhancement present	37 (57.8%)	20 (47.6%)	1.06	0.303
Heterogeneous enhancement	33 (51.6%)	16 (38.1%)	1.85	0.174
Pedicle involvement	32 (50.0%)	24 (57.1%)	0.52	0.471
Skip lesions	28 (43.8%)	21 (50.0%)	0.40	0.528
Multiple non-contiguous lesions	37 (57.8%)	22 (52.4%)	0.30	0.582
Adjacent disc sparing	28 (43.8%)	25 (59.5%)	2.52	0.112
Marrow replacement pattern	34 (53.1%)	20 (47.6%)	0.31	0.579

All comparisons were performed using the Pearson Chi-square test

MRI demonstrated low sensitivity and moderate specificity for the detection of vertebral metastases, resulting in poor overall diagnostic accuracy. Receiver operating characteristic analysis confirmed limited discriminative

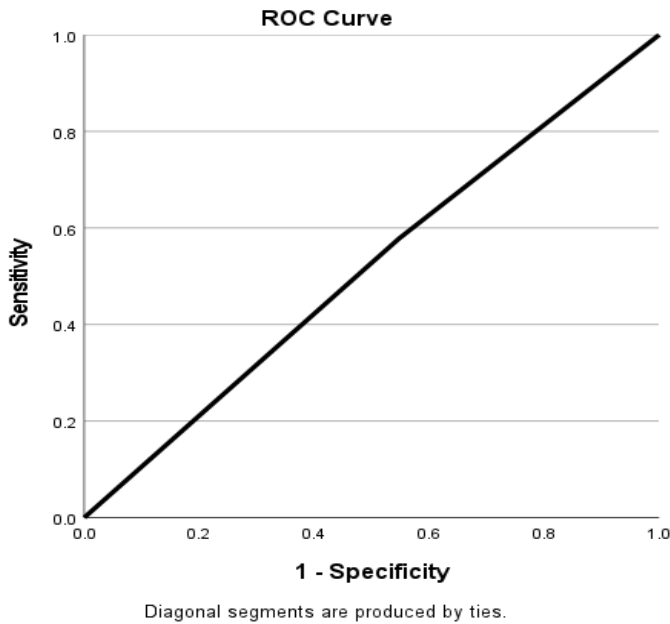


Figure 1: Receiver Operating Characteristic (ROC) Curve Showing the Diagnostic Performance of MRI for Detection of Vertebral Metastases. The Area Under the Curve (AUC) was 0.515 (95% CI: 0.40–0.63), Indicating Poor Discriminative Ability Compared with the Gold-Standard Reference

False-positive interpretations were most commonly

attributed to benign vertebral conditions such as hemangioma and infection, whereas false-negative results were mainly related to poor image quality, reader variability, and small or early marrow lesions. These findings indicate that both technical limitations and interpretative factors contributed substantially to diagnostic errors (Table 4).

Table 4: Analysis of Discordant MRI Results and Audit Findings (n=56)

Categories	n	Common reasons (Audit Findings)
False positives (FP)	19	Hemangioma (26.3%), Infection (21.1%), Other benign lesions (21.1%), Trauma (10.5%), Osteoporosis (10.5%), Modic changes (10.5%)
False negatives (FN)	37	Poor image quality (32.4%), Reader variability (21.6%), Small lesions (18.9%), Early marrow infiltration (16.2%), Other causes (10.8%)

No significant differences were observed between the metastatic and non-metastatic groups with respect to neurological deficit, need for urgent surgery, or radiotherapy planning. Length of hospital stay was also comparable between the two groups, indicating that short-term clinical outcomes did not differ significantly according to metastatic status. Effect sizes were negligible for all assessed clinical outcomes (Table 5).

Table 5: Clinical Outcomes and Management According to Vertebral Metastatic Status (n=106)

Parameters	Metastasis, n (%)	Non-metastasis (%)	Test	χ^2 (df)	p-value	Cramer's V
Neurological Deficit	32 (50.0%)	22 (52.4%)	χ^2	0.058 (1)	0.810	0.023
Need For Urgent Surgery	29 (45.3%)	21 (50.0%)	χ^2	0.224 (1)	0.636	0.046
Radiotherapy Planned	29 (45.3%)	20 (47.6%)	χ^2	0.054 (1)	0.816	0.023
Hospital Stays (Days), Median (IQR)	10 (8%)	11.5 (7%)	Mann-Whitney U	–	0.142	–

DISCUSSION

The present study evaluated the diagnostic performance of conventional 1.5-Tesla MRI interpreted by routine visual criteria for detecting vertebral metastases using histopathology and/or multidisciplinary tumor board consensus as the reference standard. MRI demonstrated low sensitivity (42.2%) and modest specificity (54.8%), with an AUC of 0.515 (95% CI: 0.40–0.63), indicating poor discriminative ability. Taken together, these findings suggest that when routine MRI interpretation is reduced to a binary “metastasis vs non-metastasis” decision based on multiple overlapping features, diagnostic separation becomes limited in real-world reporting conditions. Harlianto et al. reported that meta-analytic evidence suggests that, under optimized protocols and standardized assessment, MRI can achieve substantially higher pooled sensitivity and specificity for spinal metastases, indicating that the poor performance observed in the present cohort likely reflects real-world methodological and interpretative constraints rather than intrinsic limitations of MRI as a

modality [10]. A clinically important observation in this cohort was the high proportion of discordant scans (n=56), with more false-negative (n=37) than false-positive results (n=19). This pattern indicates that missed metastases were a larger contributor to diagnostic error than overcalling, which is relevant because false-negative interpretations may delay oncologic staging and timely intervention. The audit findings in Table 6 further clarify the mechanisms of error: false positives were commonly related to benign entities with overlapping marrow signal and enhancement (e.g., hemangioma and infection), while false negatives were linked to technical limitations (poor image quality), subtle/early marrow infiltration, small lesions, and reader-related variability. This supports the interpretation that the limited accuracy observed was not driven by a single imaging sign, but rather by the cumulative effect of overlap between benign and malignant marrow patterns under routine clinical constraints. Similar sources of diagnostic error, particularly overlap with benign marrow conditions

and limitations of visual assessment, have also been reported in comparative imaging reviews, reinforcing that misclassification remains a common challenge in routine spinal MRI interpretation [11]. When compared with contemporary literature, the performance observed in our study is lower than that reported in studies using more structured quantitative approaches or broader protocols. For example, Mijaljevic *et al.* reported very high discrimination for benign versus malignant vertebral lesions when diffusion and chemical-shift parameters were integrated, achieving an AUC close to 1.0 with high sensitivity and specificity [12]. Zhang *et al.* and Sanker *et al.* reported that, unlike our study, their diagnostic strategy relied on quantitative thresholds in addition to morphology; therefore, their results cannot be directly extrapolated to routine visual interpretation alone, but they do highlight the potential value of measurement-based workflows, and radiomics-based models have shown moderate-to-high discrimination in differentiating spinal metastases from other vertebral pathologies [13, 14]. In addition, MRI-based radiomics nomograms have demonstrated significantly improved discrimination compared with conventional morphological criteria, further supporting the concept that feature extraction beyond routine visual assessment is necessary for reliable lesion characterization [15]. Another key methodological point raised by the reviewers relates to grouping multiple MRI features into a single binary MRI outcome. In this study, MRI positivity was defined pragmatically as the presence of one or more predefined features, which mirrors real reporting practice but may dilute the individual predictive contribution of each sign. This is supported by table 4, where no single MRI feature significantly distinguished metastatic from non-metastatic lesions, suggesting substantial overlap across commonly used signal and enhancement characteristics. Therefore, the findings should be interpreted as an evaluation of routine “overall impression” MRI reporting, rather than the diagnostic power of any individual MRI parameter. This limitation of composite binary classification has also been highlighted in recent artificial intelligence and automated detection studies, where individual feature weighting and multivariate models achieved superior diagnostic separation compared with unweighted visual criteria [16, 17]. From a clinical standpoint, table 7 showed no significant difference between metastatic and non-metastatic groups in neurological deficit, urgent surgery, radiotherapy planning, or length of hospital stay. This likely reflects that treatment decisions and short-term outcomes in this cohort were influenced by multiple clinical factors (symptom burden, stability, oncologic plan), not solely by MRI classification [18]. Importantly, the

absence of group differences in these outcomes does not negate the need for accurate imaging; rather, it emphasizes that diagnostic imaging must be interpreted within a broader clinical pathway and corroborated with reference standards when uncertainty persists. Beyond initial diagnosis, MRI also plays an established role in treatment response assessment after targeted therapies such as stereotactic body radiotherapy, underscoring its broader clinical relevance in the longitudinal management of spinal metastases [19, 20].

The main strength of this study is its focus on real-world diagnostic accuracy using standard MRI protocols and routine interpretive workflows, which aligns with the journal's emphasis on practical radiology performance. This pragmatic evaluation of routine MRI performance directly aligns with the journal's scope, which emphasizes assessment of diagnostic imaging accuracy, reproducibility, and quality of radiologic interpretation in everyday clinical practice. However, several limitations should be considered. First, this was a single-center study with a moderate sample size, which may limit generalizability. Second, although MRI examinations were initially interpreted independently by two blinded radiologists, formal interobserver agreement statistics (e.g., Cohen's kappa) were not calculated; therefore, quantitative assessment of reproducibility was not performed, which may limit extrapolation to non-consensus or single-reader clinical settings. Third, the reference standard incorporated both histopathology and multidisciplinary tumor board consensus to reflect routine clinical practice; while pragmatic, this approach may introduce classification heterogeneity and partial verification bias, particularly in cases without tissue confirmation. Fourth, MRI positivity was defined using a composite visual criterion rather than feature-level diagnostic modeling; consequently, the independent predictive value of individual imaging features was not assessed, which may limit generalizability to structured or quantitative reporting frameworks. Future multicenter studies incorporating formal reproducibility analysis and feature-level modeling are warranted to validate these findings.

CONCLUSIONS

Conventional 1.5-Tesla MRI interpreted using routine visual criteria demonstrated poor diagnostic accuracy for vertebral metastases in this cohort, with low sensitivity (42.2%), modest specificity (54.8%), and poor discrimination (AUC 0.515; 95% CI: 0.40–0.63) compared with histopathology and/or multidisciplinary reference standards. Diagnostic discordance was driven predominantly by false-negative interpretations and by overlap between benign and malignant marrow patterns,

compounded by technical factors and reader variability. These findings support careful correlation with clinical context and reference standard confirmation when MRI appearances are equivocal, and they provide practice-relevant evidence aligned with the journal's scope in diagnostic radiology.

Authors' Contribution

Conceptualization: LK

Methodology: ZJO, MS

Formal analysis: TB, HB, SN

Writing and Drafting: LK, ZJO, TB, SN, MS

Review and Editing: LK, ZJO, TB, HB, SN, MS

All authors approved the final manuscript and take responsibility for the integrity of the work.

Conflicts of Interest

All the authors declare no conflict of interest.

Source of Funding

The author received no financial support for the research, authorship and/or publication of this article.

REFERENCES

- [1] Zahra SB, Majeed AI, Ehsan J. Positive Findings on Magnetic Resonance Imaging (MRI) of the Patients Diagnosed with Vertebral Metastases on Bone Scintigraphy. *Breast Cancer*. 2024 Oct; 11: 36-37.
- [2] Ahmed T, Jahan N, Sharmin F, Jahan N. Pattern of Skeletal Metastasis in Breast Cancer Patients Referred in Institute of Nuclear Medicine and Allied Sciences, Barishal. *Bangladesh Journal of Nuclear Medicine*. 2020; 23(2): 37-39. doi: 10.3329/bjnm.v23i1-2.57707.
- [3] Faiella E, Santucci D, Vertulli D, Russo F, Vadalà G, Papalia R et al. Preoperative Embolization of Vertebral Metastasis: Comprehensive Review of The Literature. *Diseases*. 2023 Aug; 11(3): 109. doi: 10.3390/diseases11030109.
- [4] Alfonso M, Llombart R, Gil L, Martinez I, Rodríguez C, Álvarez L et al. Tumor Ablation and Vertebral Augmentation in The Treatment of Vertebral Metastases: A Multicenter Study. *Revista Espanola De Cirugia Ortopedica Y Traumatologia*. 2023 Nov; 67(6): 480-486. doi: 10.1016/j.recot.2023.08.003.
- [5] Ong W, Zhu L, Zhang W, Kuah T, Lim DS, Low XZ et al. Application of Artificial Intelligence Methods for Imaging of Spinal Metastasis. *Cancers*. 2022 Aug; 14(16): 4025. doi: 10.3390/cancers14164025.
- [6] Zhan K, Chen K, Gao G, Xiang Y. A Retrospective Cohort Study on the Efficacy and Safety of Percutaneous Vertebroplasty Combined with Bone-Filling Mesh Container in Vertebral Metastases with Posterior Wall Defect. *Frontiers in Oncology*. 2024 Jan; 13: 1312491. doi: 10.3389/fonc.2023.1312491.
- [7] Tsuchiya K, Gomyo M, Katase S, Hiraoka S, Tateishi H. Magnetic Resonance Bone Imaging: Applications to Vertebral Lesions. *Japanese Journal of Radiology*. 2023 Nov; 41(11): 1173-1185. doi: 10.1007/s11604-023-01449-4.
- [8] Faiella E, Santucci D, Calabrese A, Russo F, Vadalà G, Zobel BB et al. Artificial Intelligence in Bone Metastases: A Magnetic Resonance Imaging and Computed Tomography Scan Imaging Review. *International Journal of Environmental Research and Public Health*. 2022 Feb; 19(3): 1880. doi: 10.3390/ijerph19031880.
- [9] Yang HL, Liu T, Wang XM, Xu Y, Deng SM. Diagnosis of Bone Metastases: A Meta-Analysis Comparing 18F-Fluoro-2-Deoxy-D-Glucose, Positron Emission Tomography, Computed Tomography, Magnetic Resonance Imaging, and Bone Scintigraphy. *European Radiology*. 2011 Dec; 21(12): 2604-2617. doi: 10.1007/s00330-011-2221-4.
- [10] Harlianto NI, van der Star S, Suelmann BB, de Jong PA, Verlaan JJ et al. Diagnostic Accuracy of Imaging Modalities for Detection of Spinal Metastases: A Systematic Review and Meta-Analysis. *Clinical and Translational Oncology*. 2025 May; 27(5): 2316-2326. doi: 10.1007/s12094-024-03765-1.
- [11] Ong W, Lee A, Tan WC, Fong KT, Lai DD, Tan YL et al. Oncologic Applications of Artificial Intelligence and Deep Learning Methods in Computed Tomography Spine Imaging—A Systematic Review. *Cancers*. 2024 Aug; 16(17): 2988. doi: 10.3390/cancers16172988.
- [12] Mijaljevic MB, Milosevic ZC, Lavrnic SD, Jokovic ZM, Ninkovic DI, Tubic RM et al. Assessment of Chemical-Shift and Diffusion-Weighted Magnetic Resonance Imaging in Differentiating Malignant and Benign Vertebral Lesions in Oncologic Patients. A Single Institution Experience. *Radiology and Oncology*. 2024 Oct; 58(4): 527-534. doi: 10.2478/raon-2024-0049.
- [13] Zhang S, Liu M, Li S, Cui J, Zhang G, Wang X. An MRI-Based Radiomics Nomogram for Differentiating Spinal Metastases from Multiple Myeloma. *Cancer Imaging*. 2023 Jul; 23(1): 72. doi: 10.1186/s40644-023-00585-4.
- [14] Sanker V, Gowda P, Thaller A, Li Z, Heesen P, Qiang Z et al. Applications and Performance of Artificial Intelligence in Spinal Metastasis Imaging: A Systematic Review. *Journal of Clinical Medicine*. 2025 Aug; 14(16): 5877. doi: 10.3390/jcm14165877.
- [15] Cao J, Li Q, Zhang H, Wu Y, Wang X, Ding S et al. Radiomics Model Based on MRI To Differentiate Spinal Multiple Myeloma from Metastases: A Two-

- Center Study. *Journal of Bone Oncology*. 2024 Apr; 45: 100599. doi: 10.1016/j.jbo.2024.100599.
- [16] Kim DH, Seo J, Lee JH, Jeon ET, Jeong D, Chae HD et al. Automated Detection and Segmentation of Bone Metastases on Spine MRI Using U-Net: A Multicenter Study. *Korean Journal of Radiology*. 2024 Feb; 25(4): 363. doi: 10.3348/kjr.2023.0671.
- [17] Motohashi M, Funauchi Y, Adachi T, Fujioka T, Otaka N, Kamiko Y et al. A New Deep Learning Algorithm for Detecting Spinal Metastases on Computed Tomography Images. *Spine*. 2024 Mar; 49(6): 390-397. doi: 10.1097/BRS.0000000000004889.
- [18] Daneshvar K, Shahrabaf M, Heverhagen J, Bryjova K, Aebbersold DM, Maralani PJ et al. Radiological Response Assessment After Stereotactic Body Radiotherapy for Spine Metastases Using Magnetic Resonance Imaging: A Systematic Review. *Physics and Imaging in Radiation Oncology*. 2025 Sep: 100840. doi: 10.1016/j.phro.2025.100840.
- [19] Brage K, Pedersen MR, Lauridsen CA, Paulo C, Hansen P, Precht H et al. Reporting Radiographers in CT and MRI: A Literature Review with A Systematic Approach. *Radiography*. 2025 Mar; 31(2): 102901. doi: 10.1016/j.radi.2025.102901.
- [20] Murphy L, Nightingale J, Calder P. Difficulties Associated with Reporting Radiographer Working Practices—A Narrative Evidence Synthesis. *Radiography*. 2022 Nov; 28(4): 1101-1109. doi: 10.1016/j.radi.2025.102901.